

COLLISION AVOIDANCE FOR OPERATIONAL ESA SATELLITES

H. Klinkrad¹, J.R. Alarcon², and N. Sanchez³

¹ESA/ESOC, Robert-Bosch-Strasse 5, 64293 Darmstadt, Germany

²GMV S.A., Isaac Newton 11, PTM Tres Cantos, 28760 Madrid, Spain

³Deimos Space S.A., Ronda de Poniente 19, 28760 Madrid, Spain

ABSTRACT

Since more than 10 years the European Space Operations Centre (ESOC) has been monitoring close proximities of objects of the US Space Surveillance Network Catalog with operational ESA satellites in low-Earth orbits. In recent years this activity has evolved into an operational service which is provided for the ERS-2 and Envisat remote sensing satellites. In this paper the basic principles of a Catalog based conjunction event detection and collision risk estimation process are explained, associated orbit prediction uncertainties are addressed, operational collision avoidance procedures are outlined, avoidance manoeuvre criteria are explained, and examples of evasive manoeuvres are provided. The observed manoeuvre rate is compared with a statistical manoeuvre frequency assessment, based on collision flux predictions for Catalog size objects by ESA's MASTER-2001 space debris environment model.

Key words: risk assessment; manoeuvre statistics.

1. INTRODUCTION

The first confirmed, unintentional collision between two Catalog orbits occurred on July 24, 1997, between the French Cerise satellite (95-033B) and a fragment (86-019RF) of an Ariane-1 H-10 upper stage which exploded on November 13, 1986, nine months after it delivered the SPOT-1 satellite into an orbit of $H = 826$ km at $i = 98.73^\circ$. The fragment severed the gravity gradient boom of the satellite, as could be verified by the German FGAN radar. A post-event reconstruction of the collision time matched within $\Delta t \in [0, +5 \text{ s}]$ with the time of attitude loss that was logged on board. The collision occurred on July 24, 1997, at 09:48:02 UTC, at $H = 685.8$ km, $\lambda = 59.75^\circ \text{E}$, and $\phi = 38.22^\circ \text{S}$ above the Indian Ocean. The debris object hit Cerise with a relative velocity of 14.77 km/s, under an azimuth angle of 10.5° , almost head-on (Alby et al., 1997). The French Space Agency CNES is routinely monitoring conjunction events of spacecraft operated by them (which was not so

for Cerise). Evasive maneuvers are considered, if the collision risk exceeds an accepted level of $P_c \leq 10^{-3}$.

In the United States, NASA supports collision warnings for manned missions of the Space Shuttle (STS), and of the International Space Station (ISS), based on Orbital Conjunction Messages (OCM) issued by USSTRATCOM. Different processes are applied for STS and ISS. USSTRATCOM uses general perturbation methods (analytical SGP-4 predictions) to screen the predicted orbit of ISS 72 hours ahead for Catalog object conjunctions closer than 60 km. Special perturbation techniques (numerical orbit predictions), based on osculating state vectors from USSTRATCOM are used once the conjunction is within a box of $\pm 10 \text{ km} \times \pm 40 \text{ km} \times \pm 40 \text{ km}$ ($\pm \Delta r_U \times \pm \Delta r_V \times \pm \Delta r_W$). If the event falls within $\pm 2 \text{ km} \times \pm 25 \text{ km} \times \pm 25 \text{ km}$, then covariance information on both orbits is included to assess the probability of collision (Foster, 2001). Avoidance maneuvers by ISS are considered once the near miss lies within a box of $\pm 0.75 \text{ km} \times \pm 25 \text{ km} \times \pm 25 \text{ km}$. If a maneuver decision is taken, then USSTRATCOM is informed of the post-maneuver trajectory, to verify that the new orbit does not pose a new collision risk. Based on the described process, 5 maneuvers were performed for ISS between June 1999 and May 2002.

The collision avoidance concept for the Space Shuttle (STS) is different as compared to the ISS. Based on an extensive Monte Carlo analysis of Catalog object conjunctions with STS, an alert box was defined with extensions $\pm 5 \text{ km} \times \pm 25 \text{ km} \times \pm 5 \text{ km}$ (radial \times along track \times out-of-plane), in the STS orbital coordinate system. The dimensions of this box are compatible with an accepted collision probability per event of $P_c \leq 10^{-5}$ for a Catalog population of 1988, and for typical orbit determination accuracies. Since STS-26 USSPACECOM and later USSTRATCOM were tasked to screen the STS orbits for 36 hours ahead, and raise an alert, if a conjunction event falls inside the alert box. For events within a reduced box of $\pm 2 \text{ km} \times \pm 5 \text{ km} \times \pm 2 \text{ km}$ evasive maneuvers are considered, provided that payload or mission objectives are not compromised (NASA Flight Rule A 4.1.3-6). After the Challenger accident, 61 STS missions, with 568 days on orbit, led to 6 avoidance maneuvers.

2. ORBIT PREDICTION UNCERTAINTIES

The subsequent conjunction event analysis shall focus on ESA's ERS-2 and Envisat satellites, which are operated at mean altitudes of $\bar{H} \approx 780\text{km}$, on near-circular, Sun-synchronous orbits. Different levels of accuracy are available for the orbit determination products of these satellites, depending on the user requirements, and on the accepted turn-around time. For quick-look, near real-time data, the orbit determination position accuracy over fitted observation arcs at mean atmospheric conditions is on the order of $\Delta r_{U,1\sigma} \approx 0.5\text{m}$ in radial direction, $\Delta r_{W,1\sigma} \approx 1.0\text{m}$ in out-of-plane direction, and $\Delta r_{V,1\sigma} \approx 3.0\text{m}$ in along-track direction. The corresponding velocity errors are $\Delta v_{U,1\sigma} \approx 3.0\text{mm/s}$, $\Delta v_{W,1\sigma} \approx 1.0\text{mm/s}$, and $\Delta v_{V,1\sigma} \approx 1.0\text{mm/s}$. Though these accuracies are almost two orders of magnitude worse than the best possible fits, they are still two orders of magnitude better than the presumable accuracy of the TLE data which are provided by the USSPACECOM catalog (see Table 1). Hence, when orbit determination and orbit prediction accuracy is dealt with hereafter, the focus will be on the TLE data sets.

Table 1. Assessed accuracy of TLE data for Catalog orbits with eccentricities of $e < 0.1$ and perigees of $H_{pe} \leq 800\text{km}$ (1σ uncertainties in the radial (U), transversal (V), and out-of-plane direction (W)).

pos. error (m)	$\Delta r_{U,1\sigma}$	$\Delta r_{V,1\sigma}$	$\Delta r_{W,1\sigma}$
vel. error (mm/s)	$\Delta v_{U,1\sigma}$	$\Delta v_{V,1\sigma}$	$\Delta v_{W,1\sigma}$
$i < 30^\circ$	102	419	122
	404	112	118
$30^\circ \leq i \leq 60^\circ$	129	434	163
	428	142	186
$i > 60^\circ$	104	556	139
	559	110	148

TLE data are per se not meant for precise orbit analyses. Furthermore, a metric of the quality of the orbit fit by TLE sets is not available to the normal user. To some extent, however, the latter problem can be overcome. If one assumes that a TLE data set is the best possible fit to an observed, osculating orbit over a time span of typically 36 hours Foster (2001), then one may invert the process, and conclude that a replicate of the original orbit can be reconstructed by performing a least-squares fit with a numerical propagator to a TLE-based, analytically generated SGP-4 orbit, using a realistic model of the effective perturbations. This concept is applied to 14 Catalog objects, with perigee altitudes of $338\text{km} \leq H_{pe} \leq 35,781\text{km}$, orbit eccentricities of $0.0006 \leq e \leq 0.728$, and inclinations of $4.32^\circ \leq i \leq 98.27^\circ$. For each of the 14 sample objects a 24 hour SGP-4 orbit is numerically fitted by adjusting an initial osculating state at epoch, and a drag calibration parameter. As a by-product of the batch least-squares orbit determination, an error covariance matrix is produced and stored in a look-up table for 12 different orbit categories, partitioned in 3 perigee altitude classes ($H_{pe} < 800\text{km}$, $800\text{km} \leq H_{pe} \leq 25,000\text{km}$, and $H_{pe} > 25,000\text{km}$), 3 inclination classes ($i < 30^\circ$,

$30^\circ \leq i \leq 60^\circ$, and $i > 60^\circ$), and 2 eccentricity classes ($e \leq 0.1$ and $e > 0.1$). Table 1 summarizes the 1σ uncertainties in position and velocity for near-circular LEO Catalog orbits, which are the main source of conjunction objects for ERS-2 and Envisat. The covariances C_o at epoch t_o of ascending node crossing can be propagated by means of the state transition matrix $\Phi(t_o, t)$ via

$$C(t) = \Phi(t_o, t) C_o(t_o) \Phi^T(t_o, t) \quad (1)$$

$$\Phi(t_o, t) = \partial \underline{x}(t) / \partial \underline{x}_o(t_o) \quad (2)$$

The computed 6×6 covariance matrix is extended to dimensions 7×7 by introducing an uncorrelated error of 20% (1σ) in the ballistic parameter of the object.

3. CONJUNCTION EVENT FILTER

An essential part of a collision risk assessment is the determination of near misses between pairs of space objects from the trackable Catalog population. The orbits of the ESA satellites will be assumed to be available from an operational orbit determination at epoch t_o , with resulting orbit files containing fitted and predicted states for a time span of $t \in [t_o - 2\text{d}, t_o + 8\text{d}]$, to cover (with safety margin) a typical prediction time span of +7 days. The operational satellites are hereafter denoted as targets (index "t"). They have operational orbit determination accuracies at mentioned above. The potential conjunction objects are extracted from the USSPACECOM Catalog, with recent orbit information provided in TLE format. These TLE data are propagated across the forecast time interval of +7 days, providing first order osculating states by means of USSPACECOM's SGP-4 orbit theory (the SDP-4 theory is used, if the orbital period exceeds 225 minutes). The conjunction counterparts are hereafter denoted as risk objects (index "r"). Their orbits have deduced standard deviations relative to reconstructed "true" orbits as listed in Table 1.

Different methods have been devised to determine close conjunction events between pairs of objects during a pre-defined time interval. Hoots et al. (1984) developed a theory which is based on geometric considerations (the same concept was applied for instance by Berend (1997) and Klinkrad (2001)). The conjunction detection in this case is performed by the successive application of an altitude filter, a plane geometry filter, and a phase filter. This approach is particularly useful, if the two orbits are available through an analytic orbit theory. However, the outlined detection concept for proximity events uses complex filter algorithms, with CPU-time demanding iterative root finders, and with a non-negligible risk of missing close fly-bys.

With the advent of ever increasing computer capacities alternative algorithms for conjunction event detections have become a viable alternative. The sieve algorithm of ESA's collision risk assessment software CRASS Alarcon (2002) consists of an initial altitude range filter, a crude range filter (based on maximum possible velocities) for each of the 3 coordinates of the range vector $\underline{\rho} = \underline{r}_r - \underline{r}_t$, three steps of a refined range filter (adjusted

for actual range, maximum relative acceleration, and actual relative velocity), and a final range-rate root finder to determine the time t_{tca} of closest approach for $\dot{\rho} = 0.0$. For each pair of objects these checks are performed in orbit time intervals of $\Delta t = 180s$, as a trade-off between function calls and rejection capability. The conjunction filter performance is shown in Table 2 for a spherical control volume of radius $R_c = 25km$, centered on the target object.

Table 2. Performance of filter steps for the detection of close conjunction events in the CRASS software.

Conjunction Sieve	Rejected Analyzed (%)	Passed Total (%)
altitude range	59.4	40.6
ρ_X (crude)	74.3	10.4
ρ_Y (crude)	72.9	2.8
ρ_Z (crude)	50.8	1.4
ρ (adjusted, true range)	34.5	0.92
ρ (adjusted, max. rel. acc.)	4.3	0.88
ρ (adjusted, true rel. vel.)	41.9	0.51
$\rho_{tca} (\dot{\rho} = 0.0) \leq R_c$	99.0	0.005

Due to secular effects of airdrag perturbations on the orbit period, with a resulting dominance of along-track position uncertainties, it is advantageous to define an ellipsoidal threshold surface, with its major axis in along-track direction. The CRASS program uses an ellipsoid aligned with the U_t, V_t, W_t axes, with dimensions $R_{c,U} = 10km$, $R_{c,V} = 25km$, and $R_{c,W} = 10km$, for a spherical threshold radius of $R_c \geq \max(R_{c,U}, R_{c,V}, R_{c,W})$ used in the sieve algorithms. A conjunction event falls into the ellipsoidal control volume, if $k_c^2 \leq 1$ in the following equation. Else, the event is rejected from further analysis.

$$k_c^2 = \left(\frac{\Delta r_U}{R_{c,U}} \right)^2 + \left(\frac{\Delta r_V}{R_{c,V}} \right)^2 + \left(\frac{\Delta r_W}{R_{c,W}} \right)^2 \quad (3)$$

Due to their simplicity and robustness the outlined sieve algorithms are found to be superior in their CPU time efficiency, and in their conjunction event detection capability, as compared with traditional methods.

4. COLLISION RISK ASSESSMENT

Each event which passes the criteria of the conjunction event sieve can be assessed for its collision probability relative to the target object. Several authors have developed methods to achieve this objective Foster (1992), Khutorovsky et al. (1993), Berend (1997), Alfriend et al. (1999), Klinkrad (2001), Patera (2001). All these approaches have the following assumptions in common:

- The position uncertainty can be described by a 3D Gaussian distribution.
- The target and risk object move along straight lines at constant velocities.
- The uncertainties in the velocities can be neglected.

- The target and risk object position uncertainties are not correlated.
- The position uncertainties during the encounter are constant, with corresponding covariances as at the time of closest approach.

The CRASS collision probability assessment scheme is based on the formulations by Alfriend and Akella Alfriend et al. (1999). It uses as inputs the relative position Δr_{tca} and relative velocity Δv_{tca} of the conjunction risk object with respect to the target, at the time t_{tca} of the closest approach (see Fig. 1).

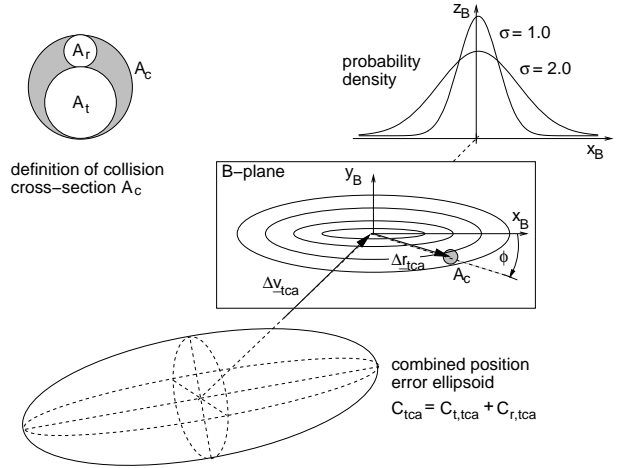


Figure 1. 2D mapping onto the B-plane of the 3D combined position uncertainty of the target and risk object at the time of closest approach (tca).

At the conjunction time t_{tca} , in accordance with the assumptions made, the propagated, uncorrelated 7×7 error covariances of the extended target and risk object state vectors can be added, to retain the upper left 3×3 combined position error covariance matrix $C(t_{tca})$.

$$C = C(t_{tca}) = C_t(t_{tca}) + C_r(t_{tca}) \quad (4)$$

This 3×3 error ellipsoid C can be mapped onto a 2×2 position error ellipse C_B in the B-plane. This B-plane contains the miss-vector Δr_{tca} , and is perpendicular to the approach velocity vector Δv_{tca} (see Fig. 1). Due to this transformation into a 2D problem, the resulting collision probability P_c can be determined from

$$P_c = \frac{1}{2\pi \sqrt{\det(C_B)}} \int_{-R_c}^{+R_c} \int_{-\sqrt{R_c^2 - x_B^2}}^{\sqrt{R_c^2 - x_B^2}} \exp[-A_B] dy_B dx_B \quad (5)$$

$$A_B = \frac{1}{2} (\Delta r_B - \Delta r_{tca})^T C_B^{-1} (\Delta r_B - \Delta r_{tca}) \quad (6)$$

Here, a circular collision cross-section of radius R_c is assumed, which surrounds the equally circular cross-sections of the risk object and the target (see Fig. 1, upper left diagram).

5. FORECAST OF MANOEUVRE STATISTICS

Mission planners and spacecraft operators would like to have forecasts of expected collision risk with cataloged and uncataloged objects before launching their satellite into a certain orbital regime. To analyse collision probabilities with Catalog objects, statistical flux results for $d > 10$ cm from ESA's MASTER-2001 model can be employed (Bendisch et al., 2002). Using a concept developed by (Foster, 2001), such collision flux results can be translated into forecasts of avoidance manoeuvre frequencies, as implemented in ESA's DRAMA software (Debris Risk Assessment and Mitigation Analysis, (Sanchez et al., 2004)).

In a first step, the flux contributing debris objects are grouped into different orbit categories, with J_H perigee altitude classes, J_e eccentricity classes, and J_i orbit inclination classes. For each of these orbit classes a mean approach direction and collision velocity is determined in the target centered, orbit related coordinate system, for J_A different azimuth classes, and J_h different elevation classes (with one class centered on $A_v = 0^\circ$ and $h_v = 0^\circ$). Impacts in the horizontal plane, between near circular orbits, are prevailing by far for large size objects in the LEO environment. As a consequence, one may assume equal orbit velocity magnitudes for both the target and risk object. With the resulting information on approach velocity and direction, corresponding B-planes for $J = J_H \times J_e \times J_i \times J_A \times J_h$ mean collision events of all orbit classes and approach directions can be defined, and the combined target and risk object position error covariance matrices can be mapped onto elliptical contours of equal collision probability in the class-specific B-plane (see Fig. 1).

Let $P_{c,acc}$ be an accepted collision probability level defined by a spacecraft operator, let the collision cross-section be defined as $A_c = (\sqrt{A_t} + \sqrt{A_r})^2$, and let the collision radius R_c be small as compared with the 1σ dimensions of the position error ellipsoid in the B-plane, then for each of the $j = 1, \dots, J$ event classes one may define contours of equal collision probability $P_c = p_c A_c$, which follow the contours of equal collision probability density p_c . If the spacecraft is maneuvered whenever the collision risk from a Catalog object exceeds the accepted level $P_{c,acc}$, then the associated rate of collision avoidance maneuvers $\dot{N}_{c,man}$ can be determined from the rate of Catalog object passes within an elliptic area defined as $P_c > P_{c,acc}$ (Foster, 2001).

$$\dot{N}_{c,man} = \sum_{j=1}^J \int_0^{A_j(P_{c,acc})} F_{j,cat} dA \quad (7)$$

where $F_{j,cat}$ is the Catalog object flux of the j -th contributing class. The corresponding reduceable collision rate $\dot{N}_{c,red}$ that can be suppressed by evasive maneuvers whenever $P_c > P_{c,acc}$ is determined from Eq. 7, weighted by a probability $P_{c,j}(\Delta r_{x,B}, \Delta r_{y,B}, R_c)$ from Eq. 5. The quantities $\dot{N}_{c,man}$ and $\dot{N}_{c,red}$ also define the false alarm probability P_{fa} , which indicates the likelihood of performing an evasive maneuver for a near-miss event that

would not have caused a collision (see Eq. 9).

$$\dot{N}_{c,red} = \sum_{j=1}^J \int_0^{A_j(P_{c,acc})} P_{c,j} F_{j,cat} dA \quad (8)$$

$$P_{fa} = 1 - \frac{\dot{N}_{c,red}}{\dot{N}_{c,man}} \quad (9)$$

Some resulting statistics shall now be reviewed for the Envisat satellite, which has a cross-section of $A_t = 530 \text{ m}^2$, and a near-circular orbit of mean altitude 784 km and inclination 98.52° (ERS-2 results can be derived by applying a scaling factor of $c_{ers} = A_{t,ers}/A_{t,env} = 0.21$).

In order to avoid unnecessary avoidance manoeuvres, one should acquire independent tracking data of the risk object, and perform orbit determinations which are more reliable and more accurate as compared to Table 1. Such tracking and orbit determination campaigns can be "simulated" by scaling the a priori risk object covariance C_r with a factor $k_{\sigma,r}$, such that

$$\hat{C}_r = k_{\sigma,r}^2 C_r \quad (10)$$

If a spacecraft operator is prepared to accept any collision risk $P_{c,acc} \leq 1.0$, then no maneuvers need to be performed ($\dot{N}_{c,man} = 0.0$), and the residual collision rate is equal to the collision rate of Catalog objects $\dot{N}_{c,red} = \dot{N}_{c,cat} = 0.00727 \text{ y}^{-1}$. In this case, the risk is invariant with pre-event warning times and orbit prediction uncertainties. Since no maneuvers are performed, the probability of false alarms is zero. If manoeuvres are performed, the false alarm rate P_{fa} grows with increasing uncertainty in the orbit determination (expressed in terms of $k_{\sigma,r}$), with decreasing levels of accepted collision probability $P_{c,acc}$, and (in general) with increasing time-to-go Δt_{tca} . Under all circumstances the execution of a manoeuvre will lead to a collision risk reduction. The effectiveness of this measure increases with decreasing time-to-go ($\eta_{c,red} = \dot{N}_{c,red}/\dot{N}_{c,cat} = 61.87\%$, 82.24% , and 93.15% for $\Delta t_{tca} = 48$ h, 24 h, and 8 h, where $P_{c,acc} = 10^{-4}$ and $k_{\sigma,r} = 1.0$), with increasing orbit determination accuracy of the risk object ($\eta_{c,red} = 93.15\%$, 97.82% , and 98.83% for $k_{\sigma,r} = 1.0, 0.1$, and 0.01 , where $P_{c,acc} = 10^{-4}$ and $\Delta t_{tca} = 8$ h), and with a decreasing level of accepted collision probability ($\eta_{c,red} = 57.14\%$ and 93.15% , for $P_{c,acc} = 10^{-3}$ and 10^{-4} , where $k_{\sigma,r} = 1.0$ and $\Delta t_{tca} = 8$ h). Hence, in order to achieve a maximum risk reduction for a small number of avoidance maneuvers, the orbit of the risk object should be improved to the same accuracy level as the well-known target orbit (typically $k_{\sigma,r} \approx k_{\sigma,t} \approx 0.01$), and the maneuver decision should be taken at the latest possible time which is compatible with operational requirements (typically $\Delta t_{tca} \approx 8$ h). Target orbit accuracies corresponding to $k_{\sigma,r} \approx 0.01$ reduce the TLE-based number of avoidance maneuvers by more than one order of magnitude from $\dot{N}_{c,man} \geq 9$ per year to $\dot{N}_{c,man} \leq 1$ in four years, for $P_{c,acc} = 10^{-4}$, with a resulting risk reduction of 98.83% . Accepting a large collision probability of $P_{c,acc} = 10^{-3}$ for this scenario causes only a minor deterioration of the risk reduction to 98.17% (only applies for small $k_{\sigma,r}$).

6. OPERATIONAL COLLISION AVOIDANCE

Since the mid 1990s ESA has been monitoring conjunction events of orbits of their remote sensing spacecraft ERS-1 (91-050A), ERS-2 (95-021A), and Envisat (02-009A) with respect to the USSTRATCOM Catalog population. During this time frame mathematical methods and operational procedures were continuously refined. The most recent development status of ESA's collision risk analysis software CRASS is documented in Alarcon (2002). In total, five evasive maneuvers were performed by ESA spacecraft: two for ERS-1 (in 1996 and 1997), one for ERS-2 (in 2004), and two for Envisat (both in 2004). The ERS-1 maneuvers were performed for a conjunction with Cosmos-614 (73-098A) at a predicted distance of $\rho_{tca} \approx 200$ m at epoch 1997/06/25 13:24:47.76 UTC, and for a near fly-by of the Hilat satellite (83-063A) at $\rho_{tca} \approx 390$ m at epoch 1998/03/21 01:42:53 UTC. Following a power failure, the ERS-1 spacecraft ceased to be operational in March 2000, after exceeding the projected mission lifetime threefold. At the same time the conjunction prediction service was discontinued, since reliable orbit data for this target were not available any more.

For all ESA missions analyzed here, an accepted collision probability of $P_c \leq P_{c,acc} = 10^{-4}$ is assumed as baseline (since the end of 2004 ESA is using $P_c \leq P_{c,acc} = 2 \times 10^{-4}$ as threshold for ERS-2 and Envisat). In a time frame between March 19 and December 27, 2004, this threshold was violated twice by ERS-2 (as compared to a prediction of 3.5 in 9 months via Eq. 8), and five times by Envisat (as compared to a prediction of 6 in 9 months). These events led to one avoidance maneuver for ERS-2, and two for Envisat. The ERS-2 maneuver was initiated after four consecutive predictions of a close conjunction with a Cosmos-3M second stage (85-079B) on days $t_{tca} - 7$ d through $t_{tca} - 3$ d. On day $t_{tca} - 3$ d the closest approach was determined for 2004/03/06 11:48:28 UTC at a distance of $\rho_{tca} \approx 170$ m, with a collision probability of $P_c = 2.63 \times 10^{-4} > P_{c,acc}$, using TLE data and applying general perturbation methods for the Cosmos-3M orbit. Based on osculating data sets and special perturbation techniques USSTRATCOM assessed the fly-by to be at a distance of 881 m, for the same epoch. In both results the conjunction location was above ERS-2, at less than 275 m vertical clearance. Hence, the ERS-2 altitude at the time of closest approach was lowered by $\Delta H_{tca} = -500$ m with two along-track burns, each of $\Delta v_V = -6.2$ cm/s, applied 2.5 and 1.5 orbits before the event, with restituting burns 0.5 and 1.5 orbits after the conjunction.

Fig. 2 illustrates the first of two Envisat avoidance maneuvers in 2004. On September 2, 2004, at 19:14:11 UTC, the Russian satellite Cosmos 1269 was predicted to pass Envisat at a distance of $\rho_{tca} \approx 1.30$ km, with a probability of collision $P_c = 2.186 \times 10^{-4}$, for a time-to-go of $\Delta t_{tca} = 1.83$ days. This high risk for a sizeable clearance is caused by a relatively oblique approach under $A_{v,tca} = 14.85^\circ$, which causes a spread of the combined position error ellipsoid along the horizontal axis within the B-plane. Due to the oblique approach geometry a fuel-efficient avoidance strategy could be chosen, apply-

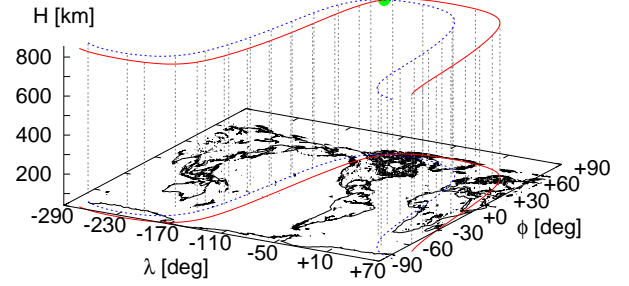


Figure 2. Conjunction event scenario for Envisat (02-009A) with the Cosmos 1269 satellite (81-041A) at epoch 2004/09/02 19:14:11 UTC.

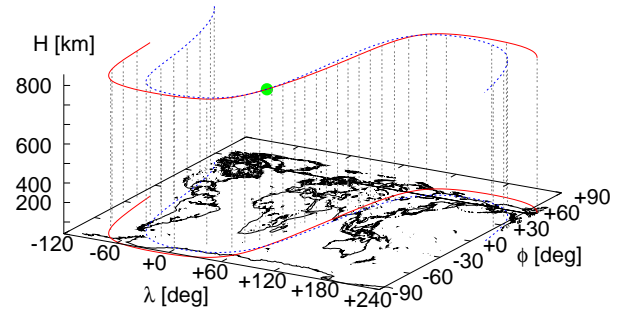


Figure 3. Conjunction event scenario for Envisat (02-009A) with a Zenith 2 upper stage explosion fragment (92-093EE) at epoch 2004/10/22 05:10:36 UTC.

ing a small along-track maneuver of $\Delta v_V = +2$ cm/s, on September 1, at 23:52 UTC, to cause a delayed arrival of Envisat at the conjunction location. The resulting increase in the conjunction distance was +1.0 km in cross-track and +75 m in radial direction for a propellant consumption of 2×80 grams (avoidance maneuver and subsequent orbit restitution maneuver).

Fig. 3 illustrates the second Envisat avoidance maneuver in 2004. During 4 consecutive predictions on days $t_{tca} - 4$ d through $t_{tca} - 1$ d a close conjunction with an explosion fragment (92-093EE) of a Russian Zenith-2 orbital stage was predicted for 2004/10/22 at 05:10:35 UTC, at distances of $81 \text{ m} \leq \rho_{tca} \leq 316 \text{ m}$, with collision probabilities of $1.4 \times 10^{-4} \leq P_c \leq 5.5 \times 10^{-4}$, all of them exceeding the accepted level of $P_{c,acc} \leq 10^{-4}$. On day $t_{tca} - 1$ d NASA verified that also on the basis of more accurate osculating state vectors provided by the SSN the conjunction distance was predicted to be in the range $150 \text{ m} \leq \rho_{tca} \leq 300 \text{ m}$. Based on the consolidated information for the conjunction event ESOC analysts and spacecraft operators prepared and up-linked a transversal avoidance maneuver of $\Delta v_V = -4.0$ cm/s (braking impulse) to be applied half a revolution (~ 50 minutes) before the conjunction, at 2004/10/22 04:20 UTC. The clearance distance in the radial direction (along the steepest gradient in the probability density) was thus increased from about 50 m to 316 m, with a corresponding reduction in the collision probability from $P_c \approx 5.5 \times 10^{-4}$ to

$P_c \approx 2.0 \times 10^{-4}$, which was considered acceptable by the project team in the view of operational constraints and required continuity in the delivery of mission products. A restituting maneuver of $\Delta V_V = +3.9$ cm/s was performed half a revolution after the conjunction, at 2004/10/22 06:00 UTC, in order to recover the ground track repeat pattern.

Whenever an avoidance maneuver is planned, as part of this process the post-maneuver trajectory is screened for new high-risk conjunction events resulting from the orbit change. This safety analysis is performed for 7.0 days ahead for ESA spacecraft, prior to taking a final avoidance maneuver decision. For ESA's ERS-2 and Envisat satellites such a screening process is also applied prior to major orbit correction maneuvers (e.g. major adjustments in the ground track repeat pattern, or inclination control maneuvers).

As of mid 2005 ESOC plans to use European tracking services (e.g. from the German FGAN, the French Monge, and the Norwegian Globus II radars) to provide data as input to ESA's dedicated ODIN software (Orbit Determination with Improved Normal equations) in the case of high-risk conjunction events. ODIN is intended to produce orbit determinations and error covariances which are typically two orders of magnitude better than information derived from TLE data sets. With the improved ephemerides and error information of the risk object orbit the mean annual manoeuvre rate for Envisat is anticipated to decrease from $\dot{N}_{c,res} \approx 8.9 \text{ y}^{-1}$ to $\dot{N}_{c,res} \approx 0.25 \text{ y}^{-1}$ for an accepted collision risk of $P_{c,acc} \leq 10^{-4}$, and from $\dot{N}_{c,res} \approx 1.8 \text{ y}^{-1}$ to $\dot{N}_{c,res} \approx 0.04 \text{ y}^{-1}$ for an accepted collision risk of $P_{c,acc} \leq 10^{-3}$, assuming a reaction time of $\Delta t_{tca} \approx 8$ h in both cases.

7. CONCLUSIONS

The European Space Operations Centre of ESA has developed an infrastructure which allows to screen flight paths of their LEO satellites for close conjunctions with objects of the USSTRATCOM Catalog. This screening process is automated, with TLE downloads, extraction of object information from the DISCOS database, conjunction event forecasts for each target object, 7 days ahead, and the issue of conjunction event protocols and warning messages to operators, if a pre-defined risk threshold is exceeded. As of mid 2005 any decision to manoeuvre will be backed up by independent, accurate ephemerides and error covariance information of the orbit of the potential collider, based on European tracking data.

ESA is conducting avoidance manoeuvres to mitigate the risk of catastrophic collisions of their ERS-2 and Envisat satellites with large size catalog objects in already densely populated altitude and inclination bands. Though such avoidance manoeuvres increase the survival probability of the spacecraft, their primary objective is to conserve the space debris environment by reducing the collision-induced proliferation of debris with mission-critical sizes, which might otherwise trigger collisional cascading in the long term.

REFERENCES

- Alfriend, K., Akella, M., Lee, D., Frisbee, J., and Foster, J. Probability of Collision Error Analysis. *Space Debris*, vol.1, no.1:21–35, 1999.
- Alarcón, J. Development of a Collision Risk Assessment Tool. Technical Report (final report) ESA contract 14801/00/D/HK, GMV S.A., Mar. 2002.
- Alby, F., Lansard, E., and Michal, T. Collision of Cerise with Space Debris. In *Proceedings of the Second European Conference on Space Debris*, ESA SP-393, pages 589–596, Mar. 1997.
- Bendisch, J., Bunte, K., Sdunnus, H., Wegener, P., Walker, R., and Wiedemann, C. Upgrade of ESA's MASTER Model. Technical Report (final report) ESA contract 14710/00/D/HK, ILR/TUBS, Braunschweig, Sep. 2002.
- Bérend, N. Étude de la Propabilité de Collision Entre un Satellite et des Débris Spatiaux. Technical Report no. RT 38/3605 SY, ONERA, Jul. 1997.
- Foster, J. A Parametric Analysis of Orbital Debris Collision Probability and Maneuver Rate for Space Vehicles. Technical Report NASA JSC-25898, NASA, 1992.
- Foster, J. The Analytical Basis for Debris Avoidance Operations of the International Space Station. In *Proceedings of the Third European Conference on Space Debris*, ESA SP-473, pages 441–445, Oct. 2001.
- Hoots, F., Crawford, L., and Roehrich, R. An Analytical Method to Determine Future Close Approaches Between Satellites. *Celestial Mechanics*, vol.33, 1984.
- Klinkrad, H. One Year of Conjunction Events of ERS-1 and ERS-2 with Objects of the USSPACECOM Catalog. In *Proceedings of the Second European Conference on Space Debris*, ESA SP-393, pages 601–611, Mar. 1997.
- Khutorovsky, Z., Boikov, V., and Kamensky, S. Direct Method for the Analysis of Collision Probability of Artificial Space Objects in LEO – Techniques, Results, and Applications. In *Proceedings of the First European Conference on Space Debris*, ESA SD-01, pages 491–508, Apr. 1993.
- Matney, N., Anz-Meador, P., and Foster, J. Covariance Correlations in Collision Avoidance Probability Calculations. *COSPAR Congress*, PEDAS1-B1.4-0038-02, Jul. 2002.
- Patera, R. General Method for Calculating Satellite Collision Probability. *Journal of Guidance, Control & Dynamics*, vol.24:716–722, Jul./Aug. 2001.
- Sánchez-Ortiz, N., Belló-Mora, M., and Klinkrad, H. Collision Avoidance Maneuvers During Spacecraft Lifetime – Analysis of Operational Missions. *55th IAC Congress*, IAC-04-IAA.5.12.5.10, Oct. 2004.